Journal of Fluorine Chemistry 130 (2009) 45–52

Contents lists available at ScienceDirect

Journal of Fluorine Chemistry

journal homepage: www.elsevier.com/locate/fluor

High temperature NMR approach of mixtures of rare earth and alkali fluorides: An insight into the local structure

Catherine Bessada *, Aydar Rakhmatullin, Anne-Laure Rollet, Didier Zanghi

CNRS-CEMHTI, 1D Av. de la Recherche Scientifique, 45071 Orleans Cedex 2, France

ARTICLE INFO

Article history:
Received 12 March 2008
Received in revised form 21 June 2008
Accepted 3 July 2008
Available online 22 July 2008

Keywords:
High temperature NMR
^{19}F
^{89}Y
Rare earth fluorides
Molten salts
EXAFS

ABSTRACT

In situ high temperature nuclear magnetic resonance in molten fluoride mixtures gives some structural picture of the complexes existing in the melt, i.e. of their nature and relative proportion. Thanks to the development of a laser heating system associated with a close crucible in boron nitride, we can describe experimentally the evolution of these complexes from the anions and the cations point of view. By ^{19}F NMR, we have shown the existence of three kinds of fluorine atoms depending on the composition: free fluorine like in pure LiF (non-bonded), bridging fluorine in melts rich in LnF_3 in addition with terminal fluorine singly bonded to one rare earth. Data obtained by NMR spectroscopy are also combined with EXAFS measurements, again thanks to a specific development of the sample holder adapted with molten fluorides and high temperature. This study is a part of our systematic investigation of the different Alk–LnF_3 systems by NMR and EXAFS spectroscopy.

1. Introduction

Lanthanide fluorides are known for their wide range of technological uses: in solid state as materials for electrodes, solid state lasers, and superionic conductors, or in the molten state in electrolytic processes for metallurgy, in pyrochemical processes for nuclear wastes recycling, or in the molten salts reactors technology [1–5]. In addition, the similarity of their chemical properties with actinides makes them particularly useful as models for the study of speciation of radioactive actinides. Pyrochemical methods for the treatment of irradiated nuclear fuel have stimulated a number of research programs and developments [3,6]. Separations would be based on the possibility of modifying the oxidation state of an element by electrolysis or by addition of a chemical agent. In a molten salt this process is complicated by different complexation phenomena and by the influence of temperature. It is of primary importance to identify the nature and the structure of the chemical species that could be involved in the reactive medium. The experimental determination of lanthanide speciation in molten fluoride media is often limited because of strong technical difficulties. These liquids are corrosive and aggressive towards a number of materials, and imply specific development of the experimental device.

Our approach is mainly based on the description of the local structure in molten fluorides by nuclear magnetic resonance (NMR) of the different observable nuclei presents in the melt. NMR spectroscopy probes the local environment around a nucleus in solid or liquid materials [7,8]. The combination of the selective information given by each nucleus, leads to the description of the melt in terms of complexes and allows determining their nature and proportion. This experimental information given by NMR spectroscopy is of primary interest to constraint the different theoretical models given for such melts.

Due to the dynamics existing in the melts, the nuclei are in rapid exchange between the different species present in the liquid and the NMR technique provides a unique tool for the description of this averaged local environment. Therefore, the signal is a single narrow peak and its position, i.e. the isotropic chemical shift, is the weighted averaged chemical shift of the different components in the melt. Knowing the chemical shift of the individual species, we can extract their distributions depending on the composition [8].

Thanks to the development of a specific heating system associating a CO_2 laser and a boron nitride crucible, we are able to work in situ on molten fluoride mixtures up to 1500 °C and to study the effect of composition, temperature, oxide content on the NMR signals of the different nuclei thus on the complexes distribution in the melt [9,7]. The only limitation would be their observability by NMR: diamagnetic, a non-zero spin, a non-negligible sensitivity.

* Corresponding author. Tel.: +33 238255509; fax: +33 238638103.
E-mail address: Catherine.bessada@cnrs-orleans.fr (C. Bessada).

0022-1139/$ – see front matter © 2008 Published by Elsevier B.V.
doi:10.1016/j.jfluchem.2008.07.010

Among the series of the lanthanide trifluorides, two families can be described depending on the ionic size of the lanthanide and the crystallographic structure at room temperature [10]. It is currently accepted that yttrium even if it belongs to the d-elements, behaves as the prototype of heavier lanthanides Ln^{3+}, from Gd to Lu, as a consequence of its ionic size and chemical behaviour. The lighters, from La to Gd, are often modelled by lanthanum.

These analogies are of great importance for NMR observation. Indeed, one of the main problems in the NMR study of lanthanides compounds is the paramagnetic properties of the trivalent lanthanide cations. The Ln^{III} have $4f^n$ ($n = 0–14$) electronic configuration. Only La^{III} and Lu^{III} have no unpaired electron and are diamagnetic, whereas the other ions in the series have 1–7 unpaired 4f ē and are thus paramagnetic. Due to the shielding of the 4f ē, the Ln^{III} ions are chemically very similar, and the different Ln^{III} complexes of a particular ligand are isostructural. Each of the Ln^{III} ions has its own characteristic effect on NMR parameters of nuclei in its proximity. The effect of these cations on both the chemical shifts and the relaxation times of the ligand nuclei can be translated into information on the molecular structure of Ln^{III} complexes. It has been exploited in NMR for a long time, especially in aqueous solutions, by the use of Ln^{III} induced shifts and relaxation enhancements for spectra simplification, and separation of overlapping NMR signals (MRI, medical diagnostic, catalysis, ...). In the case of solids it is not so common and only few experiments are reported [11,12]. The paramagnetism influences strongly the linewidth and the shifts of the observed nucleus, and can lead to unobservable signal. At high temperature in melts, because of the dynamics and the average of the different "contact" interactions, the effect is lowered and it can be possible to reach the fluorine signal in liquid containing paramagnetic nuclei, but it is still difficult and depends strongly of the complexes formed.

Different information on the structure of molten rare earth halides have been yet reported using several techniques, such as XRD, neutrons, Raman or MD, but essentially in chlorides mixtures. Pure trihalide melts are often described by octahedral coordination (LnX_6^{3-}) in which the rare earth ion is surrounded by six halide ions [13–15]. In binaries, a medium range order generated by bridging fluorines between octahedra has been described for composition rich in LnX_3. Only very few informations are known for fluorides mainly by Raman, NMR and EXAFS spectroscopy [8,16–19]. The work of G. Papatheodorou's group by Raman spectroscopy, have shown that the predominant species in molten AlkF–LnF_3 mixtures are the LnF_6^{3-} octahedra. In molten mixtures rich in LnF_3, ($X(LnF_3) < 0.25$), distorted LnF_6^{3-} octahedra are bounded by common fluorine-edges sharing. The structure of all the LnX_3 melts would be similar and independent of the structure of the solids [16,17].

Our experimental approach of the AlkF–LnF_3 binaries has been based on the systematic combination of high temperature multinuclear (^{19}F, ^{89}Y, and ^{139}La) NMR spectroscopy in melts with solid state NMR of the same nuclei on solidified AlkF–LnF_3 (Ln = La, Ce, Sm, Lu; Alk = Li, Na, K) and AlkF–YF_3 mixtures [20,21]. The ^{19}F chemical shifts sign the structural evolution from the anion point of view, and because of its great sensitivity to the local environment of the fluorine atoms it is possible to describe the network connectivity in solids, or to discriminate the bridging or non-bridging fluorines. There are several studies about ^{19}F chemical shifts calculation in inorganic solids [22–26]. From the analysis of a large number of ^{19}F isotropic chemical shifts measured in inorganic solids, with different F-sites, Bureau et al. [26] propose some empirical correlation confirmed by *ab initio* calculations, relating chemical shifts to structural parameters. They showed that fluorines can be classified into three categories: shared and unshared fluorines between two octahedra, and free fluorines which are not implied in these MF_6 octahedra. In the case of AlkF–YF_3 binaries, the yttrium fluoride structural configuration in solid compounds is not octahedral, but the description of the different kinds of fluorines is still valid and can be used to explain the chemical shift evolution in melts.

The ^{139}La and ^{89}Y NMR signals positions are directly linked to the number of fluorine atoms around the cation. The evolution of the chemical shifts measured in melts of different composition will inform on the evolution of the coordination sphere around the rare earth in the melt.

We present in this paper a review of high temperature NMR data on molten AlkF–LnF_3 binaries and more in detail some original results obtained on AlkF–YF_3 system (Alk = Li, Na, K). We focus on the information given by the ^{19}F and ^{89}Y NMR observation *in situ* in melts at high temperature and in solidified mixtures of corresponding compositions. We present also shortly the point of view of EXAFS spectroscopy in solid and liquid LiF–YF_3 system. These data will be detailed more deeply in a future paper, including spectra calculations and modelling in order to improve the information given by such technique.

2. Results and discussion

2.1. ^{19}F NMR in pure solid compounds at room temperature

At room temperature in high resolution solid state NMR experiments, the technique currently used is the magic angle spinning (MAS) technique. The rapid rotation of the sample in the field at a specific angle, 54.7° (the "magic" angle) tends to average the effect of strong interactions existing in solids, and thus to decrease the linewidths and to improve strongly the spectra resolution. In the major part of lanthanide fluorides, even in very high-speed conditions, the ^{19}F MAS spectra at room temperature on solid phases are governed by the strong paramagnetic effect of the lanthanide (Fig. 1). This effect depends on the element and is different from one cation to another. The resulting broadening can be very important such as in the case of NdF_3, with a linewidth of 300 kHz, not influenced by the spinning rate of the sample.

The ^{19}F MAS spectrum of LaF_3 at room temperature exhibits the three components at −25.2, 12.4 and 19.7 ppm (Figs. 1 and 2) corresponding to the three fluorine sites of the structure, in good agreement with the work of Wang and Grey [27] who studied the mobility of fluorine sites in connection with ionic conductivity. The

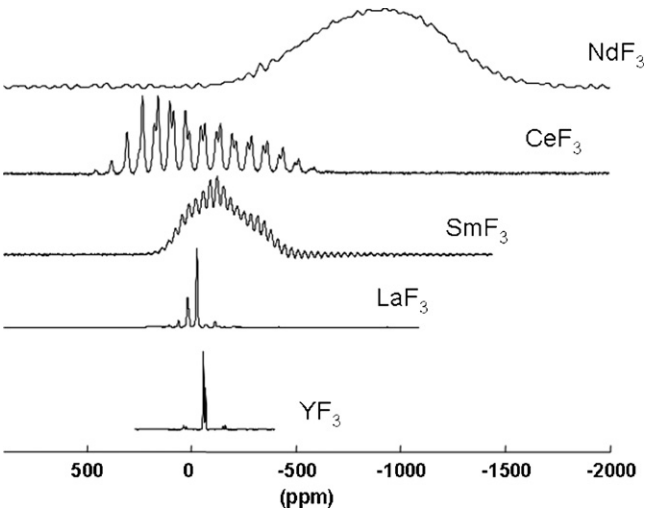

Fig. 1. ^{19}F MAS NMR spectra of solid YF_3, LaF_3, SmF_3, CeF_3, PrF_3, NdF_3 at room temperature.

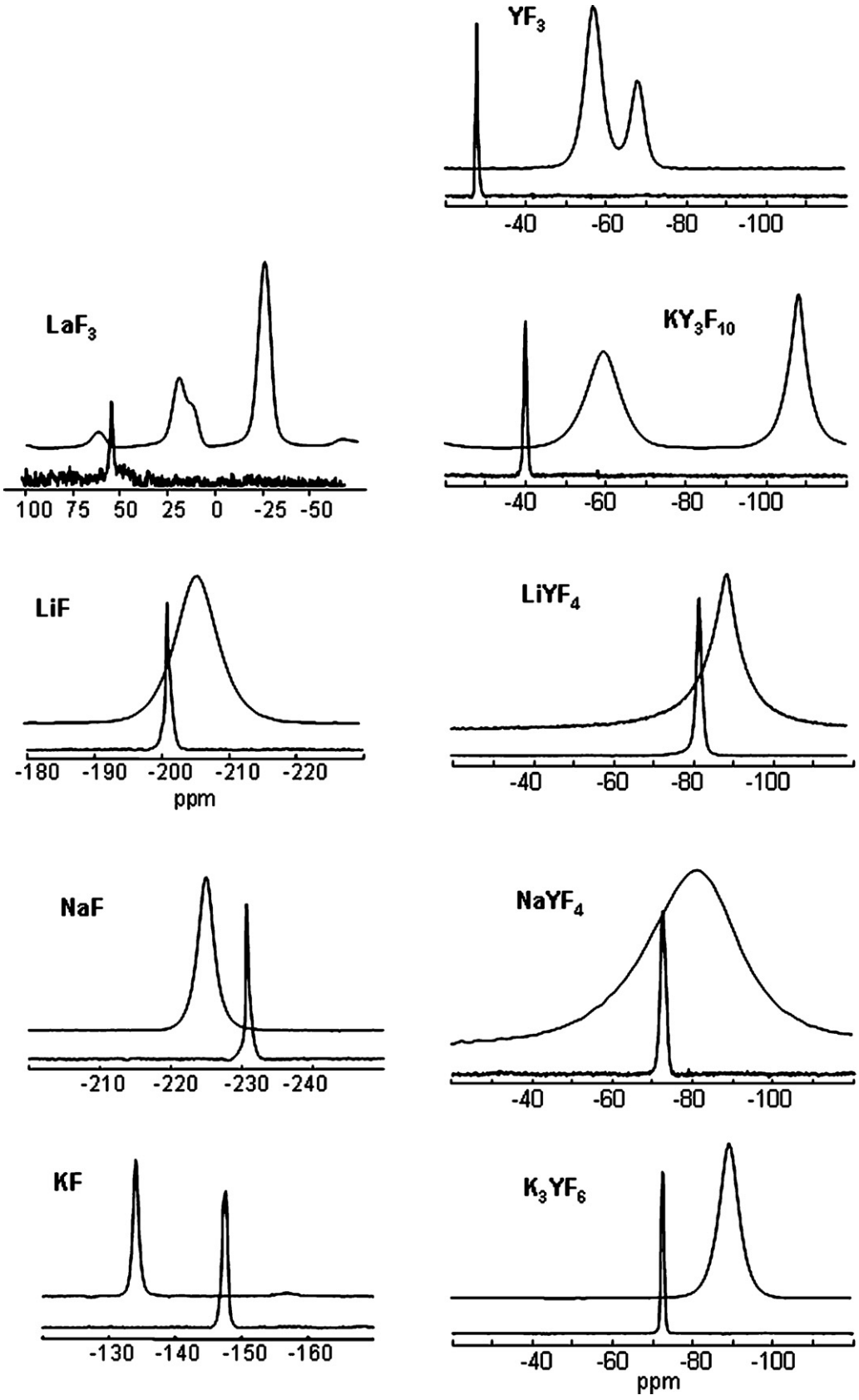

Fig. 2. Comparison between ^{19}F NMR spectra in solid (up) and melts (bottom).

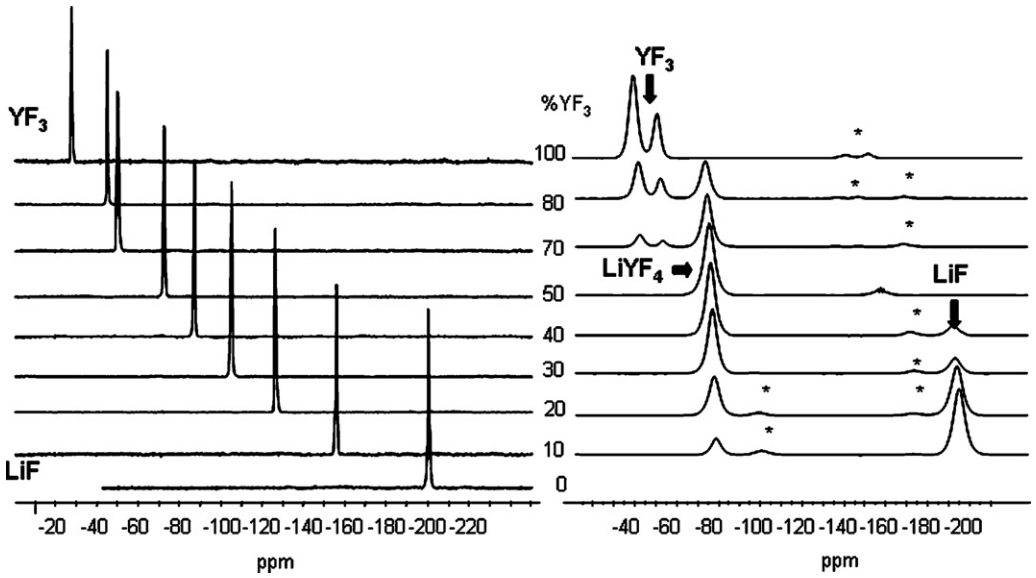

Fig. 3. (Left) High temperature ^{19}F NMR spectra evolution in YF_3–LiF melts from 0 to 100 mol% YF_3, (right) ^{19}F MAS NMR spectra at room temperature of the solidified compositions after high temperature experiments.

^{19}F MAS spectrum in YF_3 corresponds to the two different fluorine sites (F1 and F2) [28] at −67.3 and −56.3 ppm (Figs. 1 and 2). Only one fluorine site is described in the scheelite structure of $LiYF_4$ [29,30] and in general $LiLnF_4$ compounds in agreement with the spectra obtained.

2.2. NMR in Alk–LnF_3 melts

In molten Alk–LnF_3 mixtures, the ^{19}F NMR signal is a sharp and single peak as it is expected in a melt (Fig. 2). We have systematically investigated the whole range of compositions for different Alk–LnF_3 binaries 20 °C above the liquidus temperature i.e. from 800 to 1500 °C depending on the system under study. For all systems the peak is shifted from the "LiF" position at −200 ppm up to high chemical shift values at 100% LnF_3, depending on the nature of the rare earth ($^{19}F\delta = -28$ ppm in YF_3, $^{19}F\delta = 52$ ppm in LaF_3, $^{19}F\delta = -51$ ppm in LuF_3). We have observed a systematic non-linear and monotonous evolution of the ^{19}F NMR chemical shifts for several LiF–LnF_3 (Ln = La, Ce, Lu) and YF_3–LiF [8]. Nevertheless, in the case of LiF–SmF_3, the ^{19}F chemical shift was constant over the whole range of compositions [8]. This evolution could be attributed either to the presence of only free fluorine, either to a possible reduction of the samarium [31], modifying the signal detection. Consequently, the parabolic evolution of $^{19F}\delta$ seems to be a common feature of all the rare earths fluorides mixtures, except when self-reduction occurs. This evolution has been explained with the existence of three kinds of fluorines: free fluorines as in pure LiF, fluorines involved in $[LnF_x]^{3-x}$ complexes and bridging fluorines sharing different $[LnF_x]^{3-x}$ complexes. The relative concentration of each species depends on the LnF_3 content. Starting from free fluorines, the melt is enriched progressively in $[LnF_x]^{3-x}$ complexes that start to be connected for increased amounts of LnF_3, thus increasing the number of bridging fluorines in the melts. This is in agreement with the conclusions extracted from Raman spectroscopy by the group of Papatheodorou [16,17]. The point of view of the anion given by *in situ* NMR experiments confirms the important role of the fluorine in these melts. It can be noticed that this behaviour has also been observed for ThF_4–LiF melts [20].

The system with lanthanum has been carefully studied [32] and we have evidenced the strong influence of the alkali (Li, Na, K, Rb) on the local structure in the molten salt. The evolution of $^{19F}\delta$ is similar to the one described previously whatever is the alkali. It has been proposed that the amount of bridging fluorines in a given AlkF–LaF_3 mixture depends on the alkali: the more polarisable like Rb^+ the less bridging fluorines. From the point of view of ^{139}La NMR, we observed a global decrease of ^{139}La chemical shift ($^{139La}\delta$) with two domains of $^{139La}\delta$ evolution. The first one at low amount of LaF_3 (below 40%), is decreasing and parabolic that shows that there are at least three kind of lanthanum in rapid exchange LaF_x, LaF_{x+1}, LaF_{x+2}. The second one is decreasing and linear that indicates only two kinds of fluorines LaF_{x+1}, LaF_{x+2}. The analysis has shown that the average coordination around the lanthanum is increased with LaF_3 amount and tends to 8. At infinite dilution, it depends strongly on the alkali: for RbF–LaF_3 it is around 6 while it remains higher than 7 for LiF–LaF_3.

2.3. AlkF–YF_3 melts

2.3.1. ^{19}F NMR

We present in Fig. 3 the ^{19}F spectra obtained in LiF–YF_3 melts at high temperature, over the whole range of compositions, and the

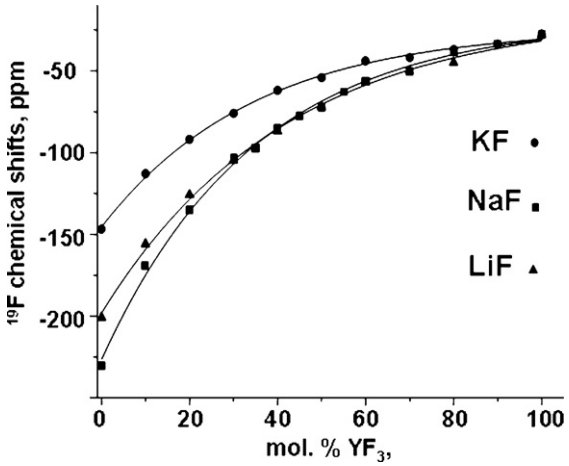

Fig. 4. ^{19}F chemical shift evolution in LiF-, NaF- and KF–YF_3 systems over the whole range of compositions.

spectra obtained at room temperature on the same compositions but solidified after high temperature experiments. The relative intensity of the different signals of LiF, YF_3 and $LiYF_4$ on each MAS NMR spectrum coincides with the proportions announced by the phase diagram [10]. It proves that the sample composition was not modified on heating. The same evolution has been observed in KF–YF_3 and NaF–YF_3.

We report in Fig. 4 the ^{19}F chemical shift evolution in the three systems over the whole range of compositions. The same trend is observed, with a monotonous but non-linear increase of the chemical shifts up to 100 mol% YF_3. As in the other system AlkF–LnF_3 described in Section 2.2 it confirms the network like structure for molten LiF–YF_3, KF–YF_3 and NaF–YF_3 systems. To go further in the description, we can compare the chemical shifts measured in the melts with those obtained for several solid compounds with known crystallographic structure.

The ^{19}F chemical shifts measured in the solid compounds of the AlkF–YF_3 binaries depend on the nature of fluorine atoms local environment. In pure LiF, the fluorine atoms are considered as free fluorines not embedded into any complex. In solid yttrium fluorides, the structure is made of $[YF_x]^{3-x}$ polyhedra more or less connected by bridging fluorines [33–37]. In solid YF_3, at room temperature, the structure is made of $[YF_9^{6-}]$ polyhedra. The bridging fluorines are connecting three yttrium atoms F(3Y), while in $LiYF_4$ [29] and $\alpha NaYF_4$ [38], all the fluorine atoms are shared between two $[YF_8^{5-}]$. In the case of KY_3F_{10}, the two kinds of fluorines are reported with a ratio 1:3, one connecting two yttrium, F(2Y) and one three yttrium F(3Y) [33]. The corresponding ^{19}F chemical shifts values measured are different: −56, −67 and −59 ppm for F(3Y) in YF_3 and KY_3F_{10} respectively, −108, −82 and −89 ppm for F(2Y) in KY_3F_{10}, $LiYF_4$ and $\alpha NaYF_4$, respectively. We can separate from these data two chemical shifts domains corresponding to the two kinds of bridging fluorine: around −60 ppm for F(3Y) and around −90 ppm for F(2Y).

In Fig. 2, the room temperature ^{19}F MAS NMR spectra of yttrium fluoride compounds (YF_3, KY_3F_{10}, $LiYF_4$, $NaYF_4$ and K_3YF_6) are compared with the sharp line obtained in the corresponding melt. We observed a systematic shift of the fluorine signal position on melting to more positive chemical shift values: 5 ppm in K_3YF_6 and up to 30 ppm in the case of YF_3.

For K_3YF_6 we have followed the ^{19}F signal measured at different temperatures, i.e. in the different polymorphs (Fig. 5). The crystallographic structure has been recently published [39] and is defined as analogous to the cryolite structure, Na_3AlF_6, with isolated YF_6^{3-} octahedra. The fluorine atoms are not bridging but connecting one yttrium and two potassium atoms. At room temperature the ^{19}F spectrum is made of only one peak, that corresponds to only one fluorine site and the chemical shift measured is −89.6 ppm. On heating, thanks to the dynamics existing in the different solid phases, the line is narrowed and we do not need to use MAS techniques, and the spectra are thus obtained in static conditions. The position is just only slightly shifted up to 910 °C and the melting is just marked by a shift of 3 ppm, and a subsequent narrowing of the signal. It proves that the effect of the temperature can be estimated to a few ppm. Consequently, in melts the evolution of the ^{19}F chemical shifts in the binary KF–YF_3 system from −150 to −30 ppm cannot be attributed to a simple effect of temperature.

We can thus propose that up to 25% YF_3, the fluorine atoms are mainly not bridging. The parabolic shape of the ^{19}F chemical shifts evolution implies that bridging fluorines are also present but in a less important proportion. This proportion will increase rapidly with the YF_3 content.

2.3.2. ^{23}Na NMR

We can also take advantage of the presence in these systems of alkali observable by NMR: ^7Li, ^{23}Na, ^{39}K. Except for ^{23}Na, up to now, we were not able to extract additional information. For ^7Li, the chemical shifts range is too small to show any structural changes around the cation and ^{39}K has a very low resonance frequency not accessible with our high temperature probe.

High temperature ^{23}Na measurements were done for the different compositions. We observe a decrease of the chemical shifts values over the whole range of YF_3 content (Fig. 6), with a plateau between 40 and 55 mol% YF_3 around the $NaYF_4$ composition. A similar evolution has been observed for NaF–LaF_3 with the plateau between 18 and 32 mol% LaF_3 centred around the eutectic composition [40,10,41]. This decrease with LnF_3 addition corresponds to an increased shielding of the alkali. Therefore the electronic cloud around Na nucleus becomes more symmetric. It means that the Na–F interaction decreases with LnF_3 amount and sodium becomes freer.

This conclusion in term of conductivity is important as the Na^+ ion would become the main charge carrier at high LnF_3 content. It

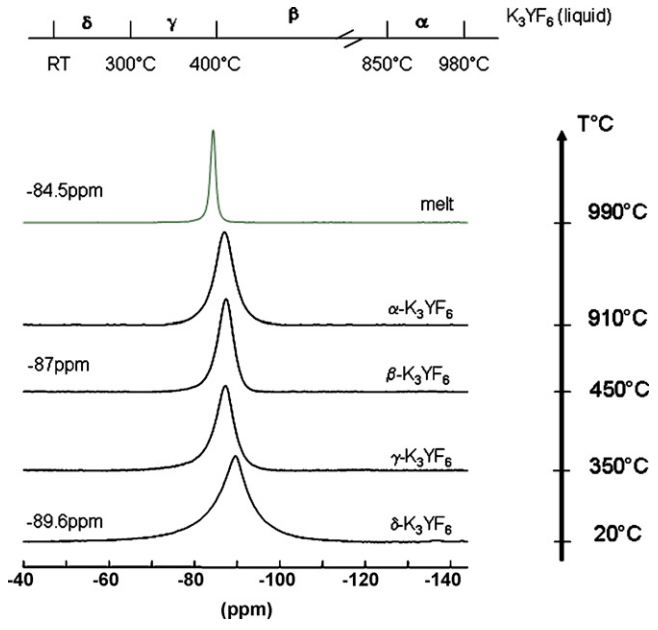

Fig. 5. ^{19}F NMR signal evolution with temperature in K_3YF_6 from the δ solid phase at room temperature up to 990 °C in the liquid.

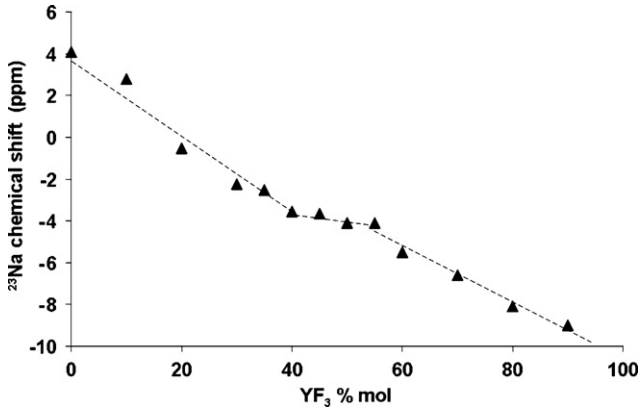

Fig. 6. ^{23}Na chemical shift evolution in NaF–YF_3 system over the whole range of compositions.

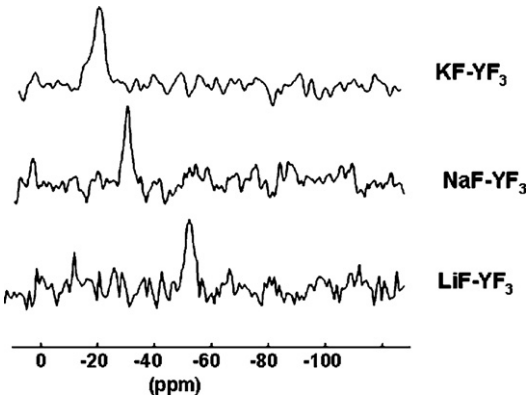

Fig. 7. ^{89}Y HT NMR spectra in Alk–YF_3 (50–50%) molten mixtures. (The spectra were acquired 10 °C above the liquidus.)

should be explored more precisely in order to give a whole description of the species formed in such melts, and their role in the conductivity properties.

2.3.3. ^{89}Y NMR

^{89}Y have low gyromagnetic ratio, γ and is characterized by a low resonance frequency. Even if this nucleus have high natural abundance (100%) and a 1/2 nuclear spin, because of its long relaxation time (several tens of minutes) it is difficult to obtain a good signal-to-noise ratio in a limited time. It can be a problem during an experiment at high temperature and we tried to find a compromise between the heating duration and the NMR detection, in other words we have tried to combine the stability of the composition and the resolution of the signal. As for the other rare earth fluorides, YF_3 is characterized by a high melting temperature (1150 °C).

Our first results have shown that the coordination of the yttrium atom was modified on melting, but remains constant over the whole set of composition in YF_3–LiF binary [8]. We have tried to improve this description by extending the domain of composition studied and looking at the effect of the alkali (Fig. 7).

In Alk–YF_3 mixtures, the ^{89}Y signal has been obtained for three different compositions 30, 50 and 70 mol% YF_3 at 1150 °C. Because of the limited duration of the high temperature experiments, the signal-to-noise ratio is poor. Nevertheless, the position of the line can be defined and depends only on the nature of the cation. It is located at −50, −30 and −20 ppm for LiF, NaF, and KF–YF_3 50–50 melts, respectively. In literature, for lanthanides trihalides–alkali halides mixtures, the coordination polyhedra proposed is LnF_6^{3-} units connected by sharing fluorine when LnF_3 content is increased in the melt. From the unique observation of the high temperature spectra we cannot argue about the exact coordination of the rare earth ion, but we can correlate the average values measured in the melt with the chemical shifts defined in solid compounds.

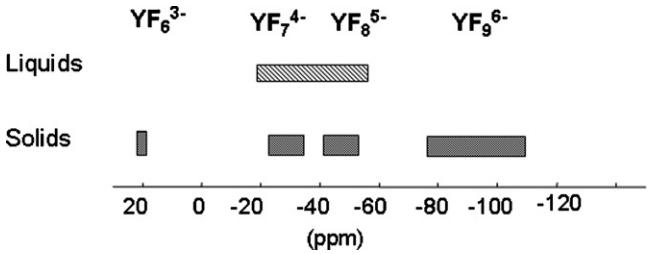

Fig. 8. ^{89}Y chemical shifts range for different $[YF_x]^{3-x}$ coordination.

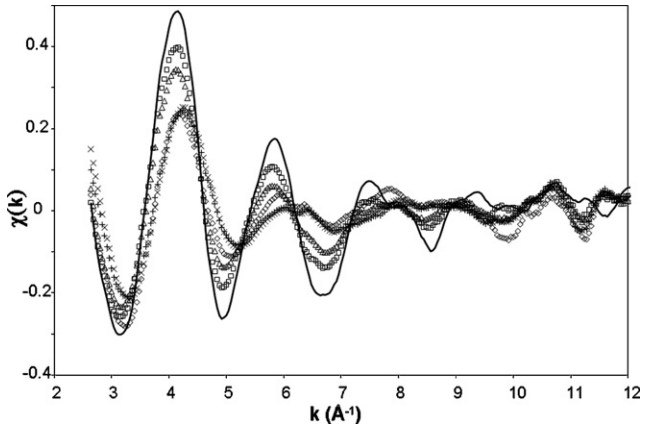

Fig. 9. Y K-edge EXAFS spectra of LiF–YF_3 10–90 mol% in the solid at room temperature (black line), at 400 °C (empty square), at 600 °C (empty triangle), in the liquid at 800 °C (cross), at 850 °C (plus sign) and of the solidified sample (dashed line) after cooling at room temperature.

In the binary KF–YF_3, we can focus on the K_3YF_6 composition. In the solid, the crystallographic structure [39] is characterized by YF_6^{3-} configuration corresponding with a ^{89}Y chemical shift at 20 ppm, while in the molten phase, the chemical shifts is moved toward −20 ppm. This evidences clearly a strong modification of the local structure around the yttrium in the melt.

We have reported in Table 1 the ^{89}Y NMR chemical shifts measured for different solid yttrium fluoride compounds and the structural parameters reported in the literature [33–38]. This set of values will help us in the interpretation of high temperature data. A simple empirical correlation between the chemical shifts measured in the solid with the coordination parameters given by the literature provides a first scale for the ^{89}Y chemical shifts in yttrium fluorides. We have reported this correspondence with the chemical shifts range measured in the different AlkF–YF_3 melts from −20 to −50 ppm in Fig. 8. The average coordination in the melts appears different from 6, and is more likely 7 or even 8 depending on the cation.

Table 1
Coordination reported for different solid yttrium fluoride compounds and the corresponding ^{89}Y NMR chemical shifts measured in solid and molten states (nm: non-measured)

Solid compounds	Polyhedron	CN	Ref.	δ^{89}Y, ppm solid	δ^{89}Y, ppm molten
YF_3	Tricapped trigonal prism	YF_9^{6-}	[37]	−112	nm
β-$NaYF_4$	2 tricapped trigonal prisms		[46]	−78, −80	
KY_3F_{10}	Square antiprism	YF_8^{5-}	[33]	−55	nm
$LiYF_4$	Capped pentagonal bipyramid		[29]	−54	−55
α-$NaYF_4$	Cubic		[38]	−44	−31
KYF_4	2 pentagonal bipyramids	YF_7^{4-}	[36]	−25, −32	−20
K_2YF_5	Capped octahedron		[34–35]	−25	−19
K_3YF_6	Octahedron	YF_6^{3-}	[39]	20.9	−20

2.4. EXAFS at the Y K-edge

EXAFS experiments have also been performed on LiF–YF_3 system at the Y K-edge. The XAFS spectra are presented in Fig. 9 from the solid to the melt at 850 °C and in the solid after cooling. The oscillation intensity decreases when temperature is increased due to the thermal agitation, but the spectra are not changed in phase or wavelength. A change occurs when the sample is melted. Moreover, the spectra at 800 and 850 °C are superimposed. It shows that the local environment around yttrium in molten LiF–YF_3 system is not sensitive to temperature. The spectrum of the solidified sample is not superimposed to the one of the initial solid because of $YLiF_4$ formation. The main result of EXAFS experiment is the decrease of the distance Y–F upon melting that must be correlated to a decrease of the coordination number. It is also linked to an increase of the interaction between yttrium and fluorines in agreement with NMR description in the case of AlkF–LaF_3 system [32].

This phenomenon has been already observed for LiF–LaF_3 [18], LiF–LuF_3 [21] and LiF–ThF_4 [20]. It seems that it is a common feature for the LiF–LnF_3 and LiF–AcF_4 systems. The treatment of these data will be improved with the help of molecular dynamics in order to extract more precisely the different structural parameters.

3. Experimental

Samples were prepared in a glove box under dried argon by mixing suitable proportions of YF_3 (Aldrich, 99.99%) and LiF, KF, NaF (Aldrich, 99.9%) without further purification. $NaYF_4$ and $LiYF_4$ were made from a mixture of 50 mol% YF_3 and the respective alkali fluorides, in a high-purity boron nitride crucible heated at 970 °C (for $NaYF_4$) and 850 °C (for $LiYF_4$) and rapidly cooled in liquid nitrogen. $LiYF_4$ and α-$NaYF_4$ structures were confirmed by X-ray analysis. A sample of K_3YF_6 of very high-purity was kindly provided by V. Dracopoulous (ICEHT-FORTH, Patras) and KYF_4, K_2YF_5 and KY_3F_{10} were synthesized by M. Body from the Laboratory of Oxides and Fluorides, Le Mans, France.

3.1. NMR spectroscopy

All NMR experiments have been carried out with a Bruker DSX 400 NMR spectrometer with a magnetic field of 9.4 T, operating at frequencies of 19.6 MHz for ^{89}Y, 105.8 MHz for ^{23}Na and 376.3 MHz for ^{19}F. High temperature (HT) NMR experiments were acquired using the previously described laser heated system developed at CRMHT (Orleans, France) [9]. Each sample was contained in a high-purity boron nitride (BN AX05 from Carborundum) crucible, tightly closed by a screwed BN cap. The crucible was placed inside the RF coil, in the centre of the cryomagnet, and heated by a continuous CO_2 laser beam (λ = 10.6 μm). A ceramic shield thermally isolated the axial saddle coil. The high temperature ^{19}F NMR spectra were obtained using single pulse excitation of 20 μs pulses; recycle delays of 500 ms, and 256 scans to obtain a reliable signal-to-noise ratio. For ^{89}Y delays were increased to 15 s for 256 accumulations. All HT NMR spectra were recorded at temperatures corresponding to 10–20° above the melting temperature of the corresponding composition.

^{19}F and ^{89}Y solid state MAS NMR spectra were obtained at room temperature on stable compounds of the AlkF–YF_3 systems, and on solidified compositions after high temperature measurements. At room temperature, ^{19}F MAS spectra have been acquired using very high-speed MAS probes from Bruker, with 2.5 mm diameter rotors allowing reaching spinning speeds of 35 kHz. Spectra were typically acquired with short pulses of 0.6 μs, recycle delays of 2 s, and 128 acquisitions. The ^{89}Y MAS NMR experiments were performed using 7 mm diameter rotors with a spinning rate of 4 kHz, pulses of 12 μs, recycle delays of 60–1200 s, and 32–512 scans. ^{23}Na and ^{19}F chemical shifts were referenced to 1 M aqueous solutions at room temperature of NaCl and $CFCl_3$, respectively. The chemical shift of ^{89}Y was referenced to the $YCl_3 \times 6H_2O$ signal as 58 ppm [42], which corresponds to a calibration versus a 1 M solution of YCl_3.

3.2. EXAFS spectroscopy

As for NMR measurements, salts were conditioned in glove box under argon. The cells used here have been designed in our laboratory especially for high temperature X-rays absorption measurements in both solid and molten lanthanide fluorides [43]. They are made of two plates of pyrolitic boron nitride (thickness 1 mm) fixed hermetically together around the sample in order to avoid any evaporation and atmosphere interaction. A pellet of sample mixed with Boron nitride powder is hosted inside an adjusted cavity (∅ 10 mm, depth 200 μm) hollowed in one plate. The cell was heated in a tubular furnace under vacuum. Due to the geometry of the furnace, in situ EXAFS spectra were recorded in a transmission mode using two Si photodiodes as detectors placed on both sides of the furnace. The heating rate was 10 K/min up to 1200 K. A more precise description has been given in a previous publication [43].

The EXAFS experiments described in this paper were performed on the H10 beamline at LURE/DCI [44] (Laboratoire pour l'Utilisation du Rayonnement Electromagnétique, Orsay, France). Spectra were obtained on the Y K absorption edge (E_0 = 17 keV) on 10–90 mol% YF_3 composition. The data analysis has been performed using the Michalovich software [45].

4. Concluding remarks

Our experimental approach by high temperature ^{19}F and ^{89}Y NMR spectroscopy in AlkF–YF_3 binaries provides a new insight of the local structure in such melts over a wide range of compositions. The species present in molten mixtures can be then described from the point of view of the anions and the cations. The ^{19}F chemical shift evolution coincides with the existence of at least three kinds of fluorines: from free fluorines at infinite dilution, fluorines connected with Y in $[YF_x]^{3-x}$ complexes and bridging fluorines at high YF_3 contents. This evolution has been systematically observed in other AlkF–LnF_3 systems as well as in Alk–ThF_4. From ^{89}Y NMR data, we can support that the average coordination around the yttrium is not 6 as it was described in the literature but more likely 7 or 8. EXAFS measurements at the Yttrium K-edge performed on molten LiF–YF_3 have confirmed the coordination decrease on melting. The treatment of the EXAFS spectra will be rapidly improved in order to extract more precise structural parameters.

Acknowledgments

The authors thank M. Body for fruitful discussions about the chemical shifts correlation in solid inorganic fluorides and for providing solid compounds. They also thank V. Dracopoulos and G. Papatheodorou for their synthesis of pure K_3YF_6 solid sample. They are also grateful for the financial support of the program PACEN-CNRS and the GDR PARIS.

References

[1] D.G. Lovering, R.J. Gale, Molten Salt Techniques, Plenum Press, New York and London, 1987.
[2] S.K. Oh, K.M. Chung, Nucl. Eng. Des. 207 (2001) 11–19.
[3] J.-M. Loiseaux, S. David, D. Heuer, A. Nutin, C. R. Phys. 3 (2002) 1023–1034.

[4] U. Gat, J.R. Engel, Nucl. Eng. Des. 201 (2001) 327–334.
[5] L. Mathieu, D. Heuer, R. Brissot, C. Garzenne, C. Le Brun, D. Lecarpentier, E. Liatard, J.M. Loiseaux, O. Meplan, E. Merle-Lucotte, A. Nuttin, E. Walle, J. Wilson, Prog. Nucl. Energy 48 (2006) 664–679.
[6] I. Kimura, Prog. Nucl. Energy 29 (1995) 445–452.
[7] V. Lacassagne, C. Bessada, P. Florian, S. Bouvet, B. Ollivier, J.-P. Coutures, D. Massiot, J. Phys. Chem. B106 (2002) 1862–1868.
[8] C. Bessada, A.-L. Rollet, A. Rakhmatullin, I. Nuta, P. Florian, D. Massiot, C. R. Chimie 9 (2006) 374–380.
[9] V. Lacassagne, C. Bessada, B. Ollivier, D. Massiot, P. Florian, J.P. Coutures, C. R. Acad. Sci. Paris, série IIb 325 (1997) 91–98.
[10] P.P. Fedorov, Russ. J. Inorg. Chem. 44 (1999) 1703–1727.
[11] E. Belorizky, P.H. Fries, L. Helm, J. Kowalewski, D. Kruk, R.R. Sharp, P.O. Westlund, J. Chem. Phys. 128 (2008) 052315.
[12] S.P. Babailov, J. Prog. NMR 52 (2008) 1–21.
[13] Y. Okamoto, T. Ogawa, Z. Naturforsch. 54a (1999) 599–604.
[14] G.M. Photiadis, B. Børresen, G.N. Papatheodorou, J. Chem. Soc. Faraday Trans. 94 (1998) 2605–2613.
[15] E. Stefanidaki, G.M. Photiadis, C.G. Kontoyannis, A.F. Vik, T. Østvold, J. Chem. Soc., Dalton Trans. (2002) 2302–2307.
[16] V. Dracopoulos, B. Gilbert, B. Borrensen, G.M. Photiadis, G.N. Papatheodorou, J. Chem. Soc. Faraday Trans. 93 (1997) 3081–3088.
[17] V. Dracopoulos, B. Gilbert, G.N. Papatheodorou, J. Chem. Soc. Faraday Trans. 94 (17) (1998) 2601–2604.
[18] A.-L. Rollet, C. Bessada, Y. Auger, P. Melin, M. Gailhanou, D. Thiaudiere, C. R. Chimie 7 (2004) 1135–1140.
[19] S. Watanabe, A.K. Adya, Y. Okamoto, N. Umesaki, T. Honma, H. Deguchi, M. Horiuchi, T. Yamamoto, S. Noguchi, K. Takase, A. Kajinami, T. Sakamoto, M. Hatcho, N. Kitamura, H. Akatsuka, H. Matsuura, J. Alloys Compd. 71 (2006) 408–412.
[20] C. Bessada, A.-L. Rollet, A. Rakhmatullin, D. Zanghi, J. Nuc. Mater. 360 (2007) 43–48.
[21] A.-L. Rollet, A. Rakhmatullin, C. Bessada, Int. J. Thermophys. 26 (2005) 1115–1126.
[22] S. Hayashi, K. Hayamizu, Bull. Chem. Soc. Jpn. 63 (1990) 913–919.
[23] U. Gross, S. Rüdiger, A.-R. Grimmer, E. Kemnitz, J. Fluorine Chem. 115 (2002) 193–199.
[24] M. Body, G. Silly, C. Legein, J.Y. Buzare, Inorg. Chem. 43 (2004) 2474–2485.
[25] M. Body, G. Silly, C. Legein, J.-Y. Buzaré, J. Phys. Chem. B 109 (2005) 10270–10278.
[26] B. Bureau, G. Silly, J.-Y. Buzaré, J. Emery, Chem. Phys. 249 (1999) 89–92.
[27] F. Wang, C.P. Grey, Chem. Mater. 9 (1997) 1068–1070.
[28] K. Rotereau, J.Y. Gesland, P. Daniel, A. Bulou, Mater. Res. Bull. 28 (1993) 813–819.
[29] E. Garcia, R.R. Ryan, Acta Cryst. C49 (1993) 2053–2054.
[30] B. Maximov, H. Schulz, Acta Crystallogr. B41 (1985) 88–91.
[31] O. Conocar, N. Douyere, J. Lacquement, J. Alloys Compd. 389 (2005) 29–33.
[32] A.-L. Rollet, S. Godier, C. Bessada, Phys. Chem. Chem. Phys. 10 (2008) 3222–3228.
[33] A. Grzechnik, J. Nuss, K. Friese, J.-Y. Gesland, M. Jansen, New Cryst. Struct. 217 (2002) 460.
[34] F. Loncke, D. Zverev, H. Vrielinck, N.M. Khaidukov, P. Matthys, F. Callens, Phys. Rev. B 75 (2007) 144427.
[35] Yu.A. Khartionov, A.Yu. Gorbunov, B.A. Maksimov, Kristallografiya 28 (1983) 1031.
[36] Y. Le Fur, N.M. Khaidukov, S. Aleonard, Acta Crystallogr., Sect. C: Cryst. Struct. Commun. 48 (1992) 978–982.
[37] L.S. Garashina, B.P. Sobolev, V.B. Alexandrov, Y.S. Vishnyakov, Sov. Crystallogr. 25 (1980) 294–300.
[38] M.D. Mathews, B.R. Ambekar, A.K. Tyagi, J. Kohler, J. Alloys Compd. 377 (2004) 162–166.
[39] M.A. Gusowki, A. Gagor, M. Trzebiatowska-Gusowka, W. Ryba-Romanowski, J. Solid State Chem. 179 (2006) 3145–3150.
[40] R.E. Thoma, H. Insley, G.M. Hebert, Inorg. Chem. 5 (7) (1966) 1222.
[41] J.P.M. van der Meer, R.J.M. Konings, D. Sedmidubsky, A.C.G. van Genderen, H.A.J. Oonk, J. Chem. Thermodyn. 38 (2006) 1260.
[42] J. Wu, T.J. Boyle, J.L. Shreeve, J.W. Ziller, W.J. Evans, Inorg. Chem. 32 (1993) 1130–1134.
[43] A.-L. Rollet, C. Bessada, Y. Auger, P. Melin, M. Gailhanou, D. Thiaudiere, Nucl. Instrum. Meth. B 226 (2004) 447–452.
[44] M. Gailhanou, J.M. Dubuisson, M. Ribbens, L. Roussier, D. Bétaille, C. Créoff, M. Lemonnier, J. Denoyer, C. Bouillot, A. Jucha, A. Lena, M. Idir, M. Bessière, D. Thiaudière, L. Hennet, C. Landron, J.P. Coutures, Nucl. Instrum. Meth. A 467–468 (2001) 745–747.
[45] A.Michalowicz, In Logiciels pour la Chimie (Software for Chemistry); Société Française de Chimie, Paris, 1991, p 102.
[46] A. Grzechnik, P. Bouvier, W.A. Crichton, L. Farina, J. Kohler, Solid State Sci. 4 (2002) 895–899.